VARIATIONS IN VENUSIAN TESSERAE: LOCAL AND GLOBAL VARIATIONS IN BACKSCATTER COEFFICIENT. J. L. Whitten[1] and B. A. Campbell[2], [1]Department of Earth and Environmental Sciences, Tulane University, New Orleans, LA, USA (jwhitten1@tulane.edu), [2]Center for Earth and Planetary Studies, National Air and Space Museum, Smithsonian Institution, Washington D.C., USA.

Introduction: The climate of Venus was likely much different in the past [1]. While most of Venus is geologically young [2] and does not preserve evidence of these ancient climate conditions, the oldest materials, known as tesserae, might. Tesserae are stratigraphically the oldest geologic unit and may have formed during a period of time with vastly different climate conditions than observed today.

Tesserae cover ~7% of the surface of Venus and appear radar bright owing to their high degree of deformation. The morphology and radiophysical properties of tesserae vary across the planet. Morphologic analyses of tesserae textures suggest significant variations within and across tesserae [3–5]. However, there has not been a global assessment of tesserae morphology (though one is currently underway [see 6]). Analysis of Magellan emissivity data indicate that there may be four major tesserae compositions, though more may exist, and their detection is limited by the variations in Magellan emissivity data [7].

Here, Magellan SAR data are analyzed in detail to determine what they reveal about the tesserae. Variations in backscatter coefficient at a small length scale (on the order of tens of kilometers) are measured to characterize differences in tesserae. Does the variability in backscatter coefficient match that observed in emissivity data? Are these variations associated with post-emplacement processes or are they associated with the original unmodified tesserae material? What does that reveal about the composition of the tesserae?

Methodology: The boundary of individual tessera deposits is mapped using Magellan SAR left look data (75 m/pixel). Backscatter coefficient values across each tesserae are derived through measurements of backslopes, ridge slopes that face away from the spacecraft during data collection. Backslopes are not saturated by the radar signal, thus providing reliable measurements of the backscatter coefficient; because the slopes face away from the radar, they are observed at higher incidence angles than the nominal boresight value for Magellan. Backscatter coefficient values are controlled predominantly by surface roughness and topography but are also affected by the composition of surfaces. Lower backscatter coefficient values are suggestive of smoother surfaces at the scale of the emitted energy (Magellan SAR had a 12.6-cm wavelength). Twenty-one major tesserae deposits were analyzed here to assess spatial trends in backscatter coefficient values. Calculated backscatter coefficient values were also compared with Magellan topography (~5 km/pixel) and emissivity (~5 km/pixel) data.

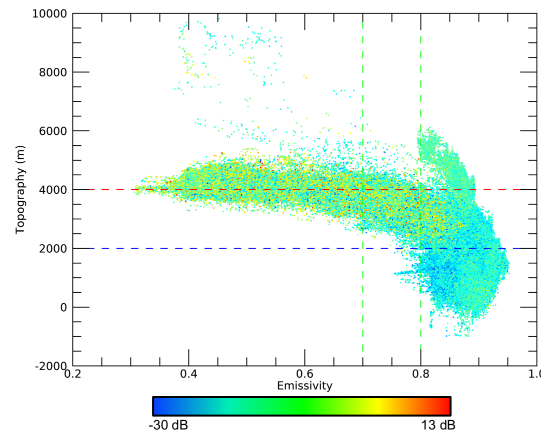

Figure 1. Backscatter coefficient data for all 21 tesserae. Dashed red line coincides with 6055 km planetary radius and the dashed blue line 6053 km. Green dashed lines coincide with boundaries defined in [7].

Results: The average backscatter coefficient for all 21 tesserae is -9.1 dB. However, backscatter coefficient values vary across the tesserae (**Fig. 1**). These values are not all dominated by changes in elevation, nor are they directly correlated with latitude or longitude. There are, however, certain regions of Venus above 6053 km planetary radius that are dominated by variations caused by elevation-controlled processes [e.g., 7, 8]. Latitudinal effects are preserved in these data, despite accounting for this variation in the backscatter coefficient calculations [9] (**Fig. 2**).

Two high-standing regions, Fortuna (+Maxwell Montes) and Thetis Regio, contain the majority of the high backscatter coefficient values (warm colors, **Fig 1**). Other tesserae, like Sudenitsa, contribute to these higher values as well. The lowest backscatter coefficient values are associated with Hyndla, Doyla, Tellus, Husbishag, and small regions of Thetis tesserae (**Fig. 2**).

Within each named tessera there are backscatter variations as well. The spread in backscatter coefficient varies, with Thetis Regio and Clotho Tessera having the largest range in backscatter coefficient (<40 dB) and Ustrecha, Cline, and Cocomama having little significant variation (with a range of ~14 dB) (**Fig. 2**).

Given that tesserae are modified by distal ejecta (i.e., parabolic ejecta) from complex craters [10, 11], the

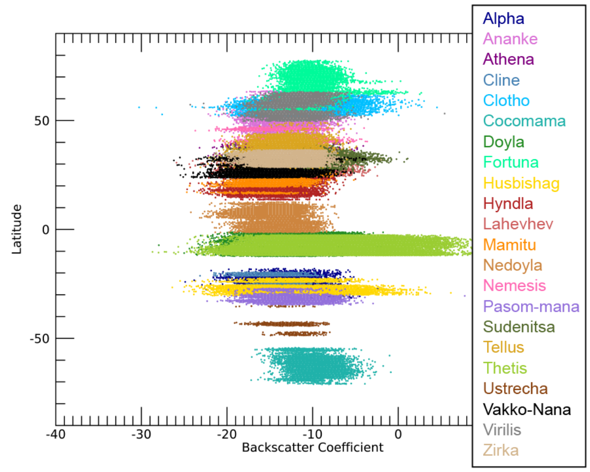

Figure 2. Backscatter coefficient as a function of latitude. A residual pattern of enhanced backscatter coefficient values is associated with lower latitudes.

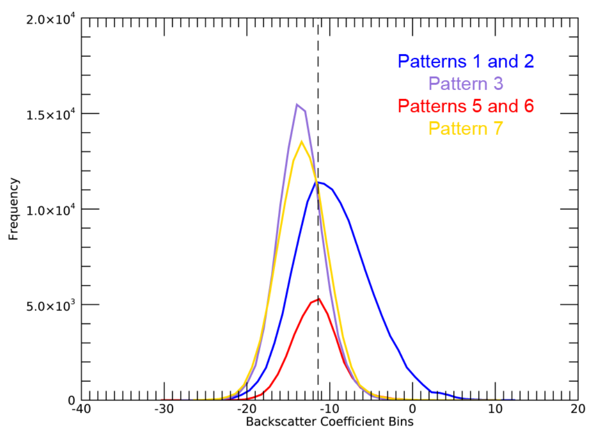

Figure 3. Histograms of backscatter coefficient for a subset of tesserae that overlap with those studied by [7]. "Patterns" are groupings of tesserae based on the emissivity measurements of [7]. Black vertical dashed line is the average backscatter coefficient value for all 21 tesserae, not just those

expected ejecta pattern around Mead crater (the largest impact structure, ~270 km in diameter) was measured. Mamitu, Vako-Nana and Tellus tesserae overlap Mead's expected ejecta parabola deposit (based on measurements of existing parabolas [12]). No spatial pattern in backscatter coefficient and expected ejecta pattern was observed.

Discussion and Conclusions: Global patterns in backscatter (**Fig. 2**) corresponding to latitude may be related to variations in the backslope angles of ridges in tesserae. The latitude correction is tied to incidence angles which would be impacted by surface slopes. Thus, the variations may reflect changes in tesserae slope distributions. Local differences in the backscatter coefficient values appear to result from emplacement of distal ejecta from complex craters [10, 11] and likely inherent differences in the tessera material properties and/or composition; significant differences in backscatter coefficient values cannot all be attributed to post-emplacement modification. There is no definitive evidence of pyroclastic materials altering backscatter coefficient values in the tesserae. Differences that cannot be associated with other geologic landforms will be compared with the surface morphology and tesserae textures [6] to determine if these variations can be ascribed to materials that could represent accretional terrains [e.g., 13] and, perhaps, indicate differences in the original composition of these tesserae materials.

Comparing these backscatter results with the emissivity results of [7] indicates that there may be some consistency between radar datasets (**Fig. 3**). Patterns 3 (Zirka, Nedoyla, Alpha, Hyndla, and Doyla) and 7 (Tellus, Cocomama, Nemesis, Athena, etc.) have similar backscatter trends, while tesserae in Patterns 1/2 (Sudenitsa and Thetis) and 5/6 (Fortuna and Clotho) have different distributions of backscatter coefficient values, with Patterns 1/2 including the radar brightest tesserae materials.

Tesserae have been thoroughly analyzed with available Magellan and Arecibo datasets over the last ~25 years. Though there is tantalizing evidence of significant differences in tesserae materials across Venus, additional data is necessary in order to definitely determine the composition of tesserae and the process(es) responsible for their formation. This fundamental information has implications for the role of water in the geologic history of Venus and may reveal different past climate conditions [1]. New *global* mission data, like that proposed by the VERITAS Discovery mission concept, is necessary to address these fundamental questions about our planetary neighbor.

Acknowledgments: All Magellan data used in this study were downloaded from the USGS Astropedia Annex website (https://astrogeology.usgs.gov/search?pmi-target=venus).

References: [1] Way M. J. et al. (2016) *GRL, 43,* 8376–8383. [2] Schaber G. G. et al. (1992) *JGR, 97,* 13257–13301. [3] Vorder Bruegge R. W. and Head J. W. (1989) *GRL, 16,* 699–702. [4] Bindschadler, D. L. and Head J. W. (1991) *JGR, 96,* 5889–5907. [5] Hansen V. L. and Willis J. J. (1996) *Icarus, 123,* 296–312. [6] Albach R. S. and Whitten J. L. (2021) *LPS LII*, this issue. [7] Brossier J. and Gilmore M. S. (2021) *Icarus, 355,* 11461. [8] Klose K. B. et al. (1992) *JGR, 97,* 16353–16369. [9] Campbell B. A. (1995) USGS Open file report 95-519. [10] Campbell B. A. et al. (2015) *Icarus, 250,* 123–130. [11] Whitten J. L. and Campbell B. A. (2016) *Geology, 44,* 519–522. [12] Schaller C. J. and Melosh H. J. (1998) *Icarus, 131,* 123-137. [13] Gilmore M. S. and Head J. W. (2018) *Planetary and Space Sci., 154,* 5–20.